Correlation Model for 3D Texture

Kristin J. Dana and Shree K. Nayar
Department of Computer Science
Columbia University
New York, NY 10027

Abstract

While an exact definition of texture is somewhat elusive, texture can be qualitatively described as a distribution of color, albedo or local normal on a surface. In the literature, the word texture is often used to describe a color or albedo variation on a smooth surface. We refer to such texture as 2D texture. In real world scenes, texture is often due to surface height variations and can be termed 3D texture. Because of local foreshortening and masking, oblique views of 3D texture are not simple transformations of the frontal view. Consequently, texture representations such as the correlation function or power spectrum are also affected by local foreshortening and masking. This work presents a correlation model for a particular class of 3D textures. The model characterizes the spatial relationship among neighboring pixels in an image of 3D texture and the change of this spatial relationship with viewing direction.

1 Introduction

While an exact definition of texture is somewhat elusive, texture can be qualitatively described as a distribution of color, albedo or local normal on a surface. In the literature, the word texture is often used to describe a color or albedo variation on a smooth surface. We refer to such texture as *2D texture*. In real world scenes, texture is often due to surface height variations and can be termed *3D texture*. Only recently has the issue of 3D texture become a topic of interest in the literature [7][14][3][5][4][17][9][15]. Our prior work on 3D texture includes [3][5] which provides measurements of 3D texture as a starting point for the investigation of texture appearance as a function of illumination and viewing direction and [4] which presents a histogram model for the class of 3D texture that is randomly rough, Lambertian, monochrome and isotropic. This work continues the development by presenting a correlation model for the same class of 3D textures to characterize the spatial relationship among pixels and the change of the spatial relationship with viewing direction.

Many texture algorithms have been developed for 2D texture analysis such as shape from texture [11][16][10], texture recognition and texture segmentation [6][18][8][12]. Most of these algorithms are based implicitly or explicitly on the power spectrum or equivalently on the correlation of image texture. For 3D texture, the correlation function of image texture changes in a complicated manner with viewing direction because of local foreshortening effects that depend on the varying local surface normal. In this work we present a model which uses surface statistical parameters to predict the change in the correlation length with viewing direction. Consider the texture images in Figure 1. This figure shows three oblique views of two surfaces at increasingly oblique viewing angles. The surfaces shown have the same image texture viewed frontally, but one surface is rough (3D texture) and the other surface is smooth (2D texture). The images of the smooth texture are simply warped versions of the frontally viewed 3D texture. Notice oblique views of the 2D and 3D texture are quite different. In particular, the oblique views of 2D texture show higher spatial frequencies and therefore a smaller correlation length than the oblique views of 3D texture. A computational model which quantifies the change in correlation length with viewing direction is

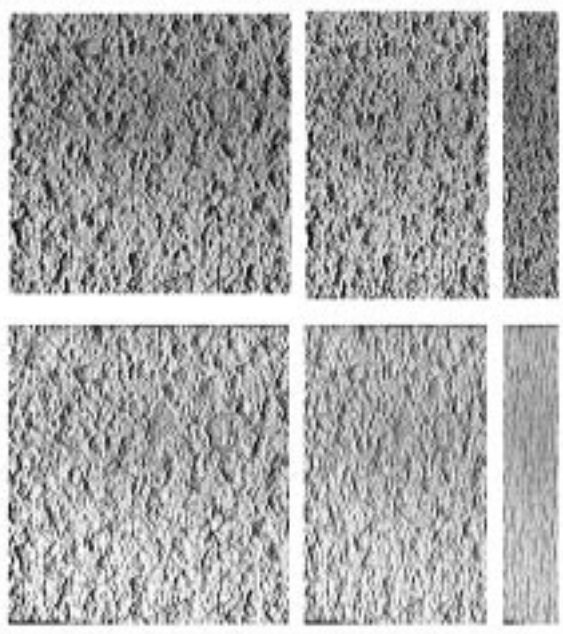

Figure 1. (Top Row) Oblique views of 3D texture. From left to right, the associated viewing angle θ_v is 33.75°, 56.25° and 78.75°. These images were obtained from a rough plaster sample of the texture database described in [5]. (Bottom Row) Oblique views of a 2D texture with θ_v varying as in top row. These views were generated by warping the frontal view of the same plaster surface. This contrived 2D texture has the same appearance in the frontal view as the rough plaster sample.

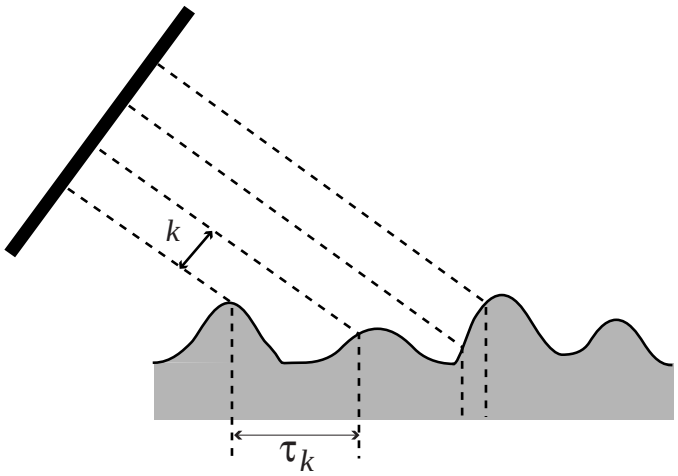

Figure 2. For a fixed distance k in the image, the corresponding surface distance is a random variable τ_k.

clearly important for algorithms which rely on spectral characteristics of texture.

2 Correlation Model

We assume that the 3D texture of interest is Lambertian and has a random height profile that can be modeled as a gaussian distribution with variance σ_h^2. We further assume that two surface points are jointly normal and the autocorrelation of the surface height process is gaussian with variance β^2. The image of this surface gives rise to an image texture. The details of the surface model are given in Appendix 5.1. In this work, we are interested in finding the correlation length of the image texture for an arbitrary illumination and viewing direction. A fixed distance k in the image corresponds to a random distance τ_k on the surface due to the varying surface profile as shown in Figure 2. Because τ_k is a random variable denoting the surface sampling, the correlation function can be written as

$$E\left(I\left[j\right], I\left[j-k\right]\right) = E\left\{E\left(I(t), I(t-\tau_k)|\tau_k\right)\right\}, \qquad (1)$$

where E denotes the expected value, $I[j]$ is the intensity for image pixel j and $I\left(t\right)$ is the intensity for the surface point at t. Note that the image intensity is written as a one-dimensional quantity for notational simplicity. To further simplify the notation let $I(t)$ and $I(t-\tau)$ be denoted by I_0 and I_τ respectively. Then the expected value can be expressed as

$$E\left(I\left[j\right], I\left[j-k\right]\right) = \int_0^\infty E\left(I_0, I_\tau|\tau_k=\tau\right) p_{\tau_k}\left(\tau\right) d\tau, \quad (2)$$

where $p_{\tau_k}\left(\tau\right)$ is the probability density function (pdf) of the random variable τ_k.

2.1 PDF of Surface Sampling

To derive p_{τ_k} we have adapted and extended the rough surface analysis given in the acoustics literature [1][19][2]

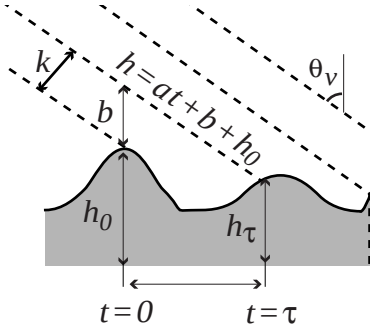

Figure 3. The probability $p_{\tau_k}\left(\tau\right) d\tau$ can be expressed as the probability the line $h = at + h_0 + b$ intersects the surface at $t = \tau$ and the surface point at $t = \tau$ is visible.

several decades ago by researchers who modeled the acoustics of a rough ocean floor. Using the law of total probability,

$$p_{\tau_k}\left(\tau\right) = \int p\left(\tau|n_0=n\right) p\left(n_0=n\right) dn, \qquad (3)$$

where n_0 is the surface normal at $t = 0$.

Let h_0 denote the surface height at $t = 0$, and let h_τ denote the height at $t = \tau$. Then,

$$\begin{aligned}&\Pr\left[\tau_k=\tau\right]\\ &= \Pr\left[\begin{array}{l}\text{surface point at } \tau \text{ is visible}\\ \text{AND } h_\tau = a\tau + h_0 + b|\ X_{v0}\end{array}\right],\end{aligned} \qquad (4)$$

where

$$\begin{aligned}a &= \tan\theta_{v,}\\ b &= \frac{k}{\sin\theta_v},\\ \theta_v &= \text{ polar angle of viewing direction,}\\ X_{v0} &= \text{ event that surface point at } t=0 \text{ is visible.}\end{aligned}$$

This situation is illustrated in Figure 3. The conditional expression is

$$\begin{aligned}&\Pr\left[\tau_k=\tau|n_0\right] =\\ &\Pr\left[\begin{array}{c}\text{surface point at } \tau \text{ is visible}\\ \text{AND } h_\tau = a\tau + h_0 + b|n_0, X_{v0}\end{array}\right].\end{aligned} \qquad (5)$$

That is,

$$\begin{aligned}&\Pr\left[\tau_k=\tau|n_0\right]\\ &= \Pr\left[X_{v\tau} \text{ AND } h_\tau = a\tau + h_0 + b|n_0, X_{v0}\right].\\ &= \int p\left(X_{v\tau}, h_0=h, h_\tau = a\tau + h + b|n_0, X_{v0}\right) dh\\ &= \int p\left(X_{v\tau}|h_0=h, h_\tau = a\tau + h + b, n_0, X_{v0}\right) \times\\ &p\left(\ h_0=h, h_\tau = a\tau + h + b|n_0, X_{v0}\right) dh,\end{aligned} \qquad (6)$$

where $X_{v\tau}$ = event that surface point at $t = \tau$ is visible.

The term $p\left(X_{v\tau}|h_0=h, h_\tau = a\tau + h + b, n_0, X_{v0}\right)$ can be found by extending the analysis of [19] and [1] as in

Appendix 5.2. The result is,

$$\begin{aligned} &p\left(X_{v\tau}|h_0=h,h_\tau=a\tau+h+b,n_0,X_{v0}\right)\\ &\approx \Pr\left(\text{surface doesn't cross the ray } a\tau+h+b \text{ in } (0,\tau)\right)\\ &=\left(\int_{M_v} p\left(n\right)dn\right)\exp\left[-\kappa\left(\begin{array}{c}\text{erf}\left(\frac{h+b+a\tau}{\sqrt{2}\sigma_h}\right)-\\ \text{erf}\left(\frac{h+b}{\sqrt{2}\sigma_h}\right)\end{array}\right)\right], \quad (7)\end{aligned}$$

where κ is a function of σ_h/β and the viewing direction and is derived in Appendix 5.2; M_v is the set of surface normals that have a positive dot product with the viewing direction.

The term $p\left(h_0,h_\tau|n_0,X_{v0}\right)$ can be expressed as

$$\begin{aligned} p\left(h_0,h_\tau|n_0,X_{v0}\right) &= \frac{p\left(X_{v0}|h_0,h_\tau,n_0\right)p\left(h_0,h_\tau,n_0\right)}{p\left(n_0,X_{v0}\right)}\\ &= \frac{p\left(X_{v0}|h_0,n_0\right)p\left(h_0,h_\tau,n_0\right)}{p\left(X_{v0}|n_0\right)p\left(n_0\right)}\\ &= \frac{p\left(X_{v0}|h_0,n_0\right)p\left(h_0,h_\tau|n_0\right)}{p\left(X_{v0}|n_0\right)}\\ &= \frac{\exp\left(\frac{-B(1-\text{erf}(h_0))}{\sqrt{2}\sigma_h}\right)p\left(h_0,h_\tau|n_0\right)}{q_v}, \end{aligned} \quad (8)$$

for $n_0\in M_v$, where we use the following results from [19]

$$p\left(X_{v0}|h_0,n_0\right)=\exp\left(\frac{-B\left(1-\text{erf}\left(h_0\right)\right)}{\sqrt{2}\sigma_h}\right), \quad (9)$$

$$p\left(X_{v0}|n_0\right)=q_v. \quad (10)$$

The terms B and q_v are derived in [19] and are a function of the surface statistics and viewing direction. Putting it all together and letting

$$\nu=\left(\int_{M_v} p\left(n\right)dn\right)/q_v,$$

we have

$$\begin{aligned} &p\left(\tau|n_0\right)=\\ &\int p\left(X_{v\tau}\ |h_0=h,h_\tau=a\tau+h+b,n_0,X_{v0}\right)\times\\ &p\left(\ h_0=h,h_\tau=a\tau+h+b|n_0,X_{v0}\right)dh\\ &=\nu\int_0^\infty \exp\left[-\kappa\left(\begin{array}{c}\text{erf}\left(\frac{h+b+a\tau}{\sqrt{2}\sigma_h}\right)-\\ \text{erf}\left(\frac{h+b}{\sqrt{2}\sigma_h}\right)\end{array}\right)\right]\times\\ &\exp\left(\frac{-B\left(1-\text{erf}\left(h\right)\right)}{\sqrt{2}\sigma}\right)p\left(h_0,h_\tau|n_0\right)dh. \end{aligned} \quad (11)$$

So,

$$\begin{aligned} &p_{\tau_k}\left(\tau\right)d\tau=\int p(\tau|n_0=n)p(n_0=n)dnd\tau\\ &=\nu\int\int_0^\infty \exp\left(\begin{array}{c}-\kappa\left(\begin{array}{c}\text{erf}\left(\frac{h+b+a\tau}{\sqrt{2}\sigma_h}\right)-\\ \text{erf}\left(\frac{h+b}{\sqrt{2}\sigma_h}\right)\end{array}\right)-\\ B\left(1-\text{erf}\left(\frac{h+b+a\tau}{\sqrt{2}\sigma_h}\right)\right)\end{array}\right)\times\\ &\exp\left(-\xi h^2-\gamma h-\eta\right)dh\ dn\ d\tau\ , \end{aligned} \quad (12)$$

where

$$\exp\left(-\xi h^2-\chi h-\eta\right)=p\left(h_0=h,h_\tau=h+b+a\tau,n_0=n\right). \quad (13)$$

The parameters ξ,χ and η are readily derived from the multivariate normal surface model. The resulting integral is too complicated to solve analytically and is evaluated using numerical integration.

2.2 Examples of $p_{\tau_k}\left(\tau\right)$

The sampling on the surface varies with the local height variations on the surface. When the viewing ray intersects uphill (positive sloped) portions of the surface, the distance between samples is small. On the other hand, when the viewing ray intersects downhill (negative sloped) portions of the surface, the sampling distance is large. In addition, peaks on the surface cause neighboring surface points to be occluded and therefore the corresponding sampling distance is large. In this section we look at several examples of the predicted sampling distance pdf p_{τ_k} as derived in the previous section.

Figure 4 shows the simulated surface for four different combinations of σ_h and β. These simulated surfaces are provided only as a reference to interpret the sampling pdf examples and were not used in the calculations. Figure 5 shows the predicted values of p_{τ_k} for $k=1,2,3$ and $\theta_v=33.75°$. Consider the characteristics of each curve. In example A of Figure 5, where σ_h is low and β is low, the sampling distance has a mean value at $k/\cos\theta_v$ and has approximately equal distribution of sample values lower and heigher than this mean value. As k increases, p_{τ_k} shows very little change with the exception of its mean value. To see that this behavior is expected, consider the corresponding simulated surface shown in example A of Figure 4. For this viewing direction, there are very few occlusions and the area of uphill points projected to the image are approximately equal to the area of downhill points. Therefore we expect an equal distribution of the curve p_{τ_k} around the mean. The value of the mean is what we expect; it is the sampling distance that would occur in the limit as σ_h goes to zero or β goes to ∞ and the rough surface becomes smooth.

In example B of Figure 5, with its corresponding simulated surface shown in Figure 4, the value of σ_h is low but the value of β is large. Because of this relatively large correlation distance, the surface is smoother and there is less variation of τ_k, i.e. p_{τ_k} has a smaller variance than example A. Also, small values of k are likely to correspond to values of τ_k that are within the correlation length and therefore p_{τ_k} for smaller k values have a smaller variance.

Example C of Figure 5, corresponds to large σ_h and small β. In this case there are significant occlusions from tall surface points. The length of the occluding mask varies causing a large variation of τ. For smaller k values, there is more of a chance of intersecting an uphill portion of the surface so the curve has more weight at low τ values.

In example D, which corresponds to large σ_h and large β, the curves for p_{τ_k} are similar to those of example B with the exception of a large variation of τ around the means caused by a larger value of σ_h.

Figure 6 shows the same examples with a more oblique viewing direction, $\theta_v=56.25°$. The plots are similar to

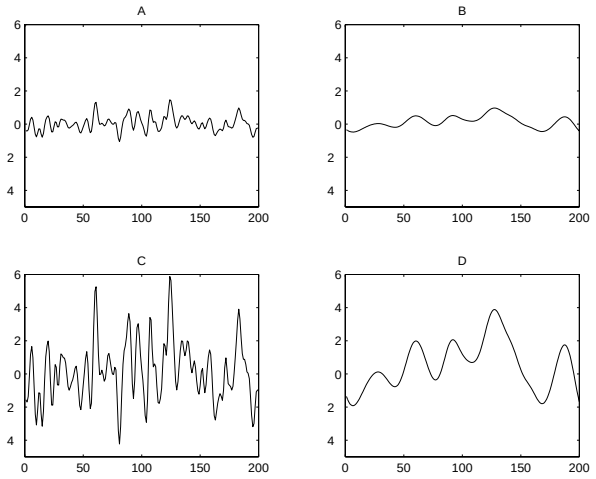

Figure 4. Four one dimensional surfaces provided for illustration purposes. A: $\sigma_h = 0.5, \beta = 1$. B: $\sigma_h = 0.5, \beta = 5$. C: $\sigma_h = 2, \beta = 1$. D: $\sigma_h = 2, \beta = 5$.

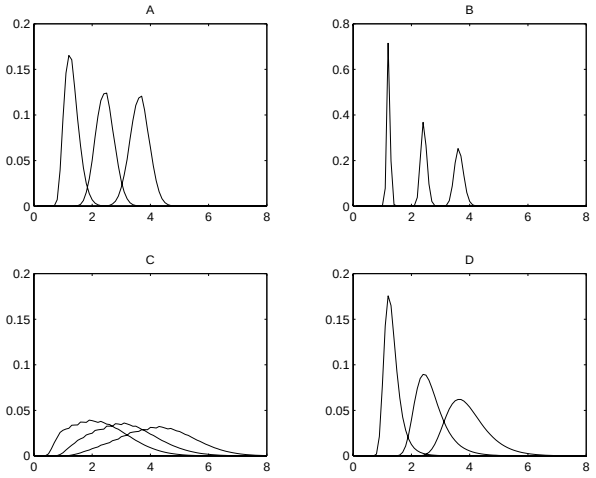

Figure 5. Four examples of p_{τ_k} obtained from the derived model with $\theta_v = 33.75^\circ$ and $k = 1, 2, 3$. A: $\sigma_h = 0.5, \beta = 1$. B: $\sigma_h = 0.5, \beta = 5$. C: $\sigma_h = 2, \beta = 1$.D: $\sigma_h = 2, \beta = 5$.

those shown in Figure 5 with the exception that the occlusions from tall surface points are large at the oblique angles causing much larger τ values to be significantly probable.

These plots show the correct behavior by qualitative arguments. In addition, during model development the predicted pdf of τ_k was compared to a computed version obtained by ray-tracing simulated surfaces. There was a good correspondence between the model predictions and these simulations.

2.3 Correlation Length

Let the correlation length of the surface be τ', so that when $\tau_k > \tau'$,

$$E\left(I_0, I_\tau | \tau_k = \tau\right) = 0.$$

We see from Equation 2 that if

$$p_{\tau_k}\left(\tau\right) = 0 \text{ for } \tau < \tau',$$

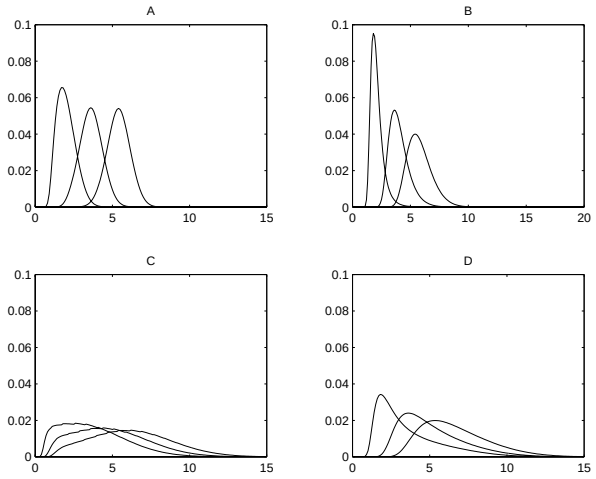

Figure 6. Four examples of p_{τ_k} obtained from the derived model with $\theta_v = 56.25^\circ$ and $k = 1, 2, 3$. A: $\sigma_h = 0.5, \beta = 1$. B: $\sigma_h = 0.5, \beta = 5$. C: $\sigma_h = 2, \beta = 1$. D: $\sigma_h = 2, \beta = 5$.

then

$$E\left(I\left[j\right], I\left[j-k\right]\right) = 0.$$

Let L be the value such that

$$p_{\tau_k}\left(\tau\right) = 0 \text{ for } \tau < \tau' \text{ whenever } k > L. \tag{14}$$

This value of L is the correlation length in the image, i.e.

$$E\left(I_0, I_k\right) = 0 \text{ when } k > L. \tag{15}$$

We note that L is a function of the viewing direction and the surface statistics. The correlation length is not independent of illumination direction in the presence of cast shadows. However if cast shadows are not dominant and the correlation is computed using only non-shadowed pixels, the resulting correlation length is equal to L.

While the random variable τ_k is not directly observable from the image, $E\left(I_0, I_k\right)$ and therefore L can be estimated from the image. The estimated values of L can be used to estimate surface statistics from a set of images obtained with known viewing direction but unknown illumination direction. Conversely, if the surface statistics are known the viewing direction can be estimated using the value of L obtained from the image.

3 Results

We employ the texture images obtained from the publicly available database described in [5]. Figure 7 shows the images of rough plaster taken under 9 different illumination and viewing directions. From left to right, the columns correspond to $\theta_v = 33.75^\circ, 56.25^\circ$ and 78.75°. From top to bottom the illumination polar angle is $\theta_s = 11.25^\circ, 33.75^\circ$ and -11.35°. For the images in each row the correlation length was computed and plotted as a function of θ_v in Figure 8 (dashed lines). Using the correlation lengths we estimated the value of σ_h and β for this surface as $\sigma_h = 0.57$ and $\beta = 1.16$. The corresponding model estimate of the correlation length L is shown in Figure 8. Also shown in this figure is the correlation length for a planar

Figure 7. Images of rough plaster (sample 11 in the texture database) taken under 9 different illumination and viewing directions. From left to right the columns correspond to $\theta_v = 33.75^\circ, 56.25^\circ$ and 78.75°. From top to bottom the illumination polar angle is $\theta_s = 11.25^\circ, 33.75^\circ$ and -11.35°.

surface (2D texture). There are two important things to notice here. First, the measured correlation length as a function of viewing direction is similar for all three illumination directions considered. Second, the model does a good job predicting the correct value of the correlation length especially when compared to the prediction obtained by assuming 2D texture.

4 Conclusion/Summary

For image understanding in real world scenes, algorithms and models which handle 3D texture are becoming increasingly important. In [4], we developed a histogram model for 3D texture that predicts the histogram of image intensities as a function of viewing and illumination direction. Using the histogram model, we estimated surface roughness from a series of images taken under different illumination and viewing directions. However, the histogram does not provide information on the spatial relationship of image pixels and the estimated surface roughness does not reveal the spatial relationship of surface points. The new model presented here allows the prediction of correlation length as a function of viewing direction. From a series of images we've estimated both surface roughness and surface correlation. Consequently, the model is used to determine the spatial relationship of image pixels and surface points.

5 Appendix

5.1 Surface Statistics

We assume the height of the surface is a gaussian random variable, i.e. the pdf of the height p_h has a standard deviation σ_h and is given by

$$p_h = \frac{1}{\sqrt{2\pi\sigma_h^2}} \exp\left(-\frac{(h-m_h)^2}{2\sigma_h^2}\right).$$

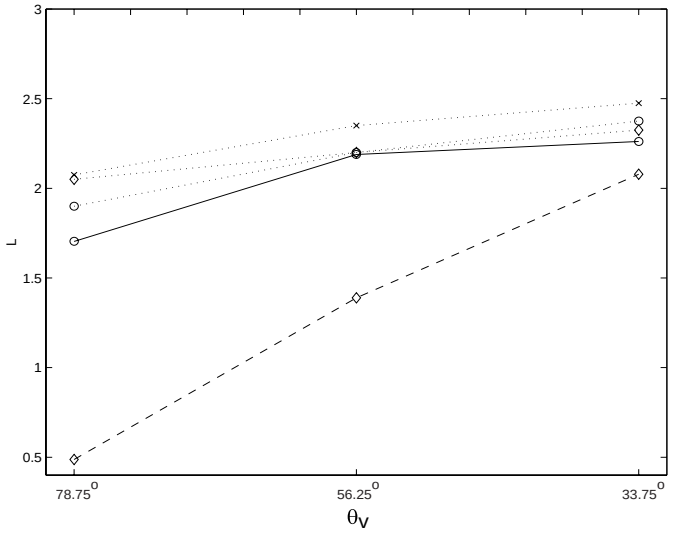

Figure 8. Measured and modeled correlation lengths. The dotted lines show the measured correlation length L as a function of $\theta_v = 33.75^\circ, 56.25^\circ$ and 78.75°. Each dotted line corresponds to a different illumination direction $\theta_s = 11.25^\circ, 33.75^\circ, -11.25^\circ$.The solid line corresponds to the model of the correlation length using the parameters that best match the measurements: $\sigma_h = 0.57$ and $\beta = 1.16$. The dashed line shows the correlation length that would be predicted if we assume the texture is a 2D texture.

We assume the correlation function is gaussian with a standard deviation of β, i.e.

$$E\left(h\left(x_1,y_1\right), h\left(x_2,y_2\right)\right) = \sigma_h^2 \exp\left(\frac{-\left(x_1-x_2\right)^2 - \left(y_1-y_2\right)^2}{2\beta^2}\right).$$

5.2 Ray Crossing PDF

In this section we've adapted our notation to be more consistent with [19]. According to the development in [19],

$$\Pr\left(\text{surface doesn't cross the ray } a\tau+\delta \text{ in } (0,\tau)\,|\delta,\delta'\right) = C\exp\left[\begin{array}{c} -\int_0^\tau \frac{1}{2\pi\sigma_h\sigma}\times \\ \int_{\eta_0}^\infty (\eta-\eta_0)\exp\left(-\frac{(\delta+\eta_0\tau)^2}{2\sigma_h^2} - \frac{\eta^2}{2\sigma^2}\right)d\eta \end{array}\right],$$

where η_0 is the slope of the viewing ray, δ is the height of the surface, δ' is the slope of the surface, $\sigma = \sigma_h/\beta$, and C is the unit step function

$$C = u\left(\eta_0 - \delta'\right) = \begin{array}{l} 1 \text{ if } \delta' \geq \eta_0 \\ 0 \text{ otherwise.} \end{array}$$

Therefore,

$$\Pr\left(\text{surface doesn't cross the ray } a\tau+\delta \text{ in } (0,\tau)\,|\delta,\delta'\right) = C\exp\left[\begin{array}{c} -\int_0^\tau \frac{1}{2\pi\sigma_h\sigma}\int_{\eta_0}^\infty (\eta-\eta_0)\times \\ \exp\left(-\frac{(\delta+\eta_0\tau)^2}{2\sigma_h^2} - \frac{\eta^2}{2\sigma^2}\right)d\eta d\tau \end{array}\right]$$

$$= C\exp\left[-\int_0^\tau \frac{1}{2\pi\sigma_h\sigma} A\exp\left(-\frac{\left(\delta+\eta_0\tau'\right)^2}{2\sigma_h^2}\right)d\tau\right],$$

where

$$A = \begin{pmatrix} -\sqrt{2\pi}\sigma\eta_0 + \sigma\sqrt{2\pi}\,\mathrm{erf}\left(\frac{1}{\sqrt{2}\sigma}\eta_0\right)\eta_0 \\ +2\sigma^2 \exp\left(-\frac{\eta_0^2}{2\sigma^2}\right) \end{pmatrix}.$$

Because

$$\int_{\eta_0}^{\infty} (\eta - \eta_0) \exp\left(-\frac{(\delta + \eta_0\tau)^2}{2\sigma_h^2} - \frac{\eta^2}{2\sigma^2}\right) d\eta =$$
$$= A \exp\left(-\frac{(\delta + \eta_0\tau')^2}{2\sigma_h^2}\right),$$

the integral can be evaluated as follows

$$-\frac{1}{2\pi\sigma_h\sigma}\int_0^{\tau}\left(A\exp\left(-\frac{(\delta+\eta_0\tau')^2}{2\sigma_h^2}\right)\right)d\tau'$$
$$= -\frac{1}{2}\sqrt{2\pi}\sigma_h A\frac{-\mathrm{erf}\left(\frac{\delta+\eta_0\tau}{\sqrt{2}\sigma_h}\right)+\mathrm{erf}\left(\frac{1}{\sqrt{2}\sigma_h}\delta\right)}{\eta_0}$$
$$= \left(\frac{1}{\sqrt{2\pi}}\frac{\sigma}{\eta_0}e^{-\frac{1}{2}\frac{\eta_0^2}{\sigma^2}} - \frac{1}{2}\left(1-\mathrm{erf}\left(\frac{\eta_0}{\sqrt{2\sigma^2}}\right)\right)\right)\times$$
$$\left(-\mathrm{erf}\left(\frac{\delta+\eta_0\tau}{\sqrt{2}\sigma_h}\right)+\mathrm{erf}\left(\frac{\delta}{\sqrt{2}\sigma_h}\right)\right).$$

So the result is

$$\Pr\left(\text{surface doesn't cross the ray } a\tau+\delta \text{ in } (0,\tau)\,|\delta,\delta'\right)$$
$$= C\exp\left[\begin{array}{c}\left(\frac{1}{\sqrt{2\pi}}\frac{\sigma}{\eta_0}e^{-\frac{1}{2}\frac{\eta_0^2}{\sigma^2}} - \frac{1}{2}\left(1-\mathrm{erf}\left(\frac{\eta_0}{\sqrt{2\sigma^2}}\right)\right)\right)\times \\ \left(-\mathrm{erf}\left(\frac{\delta+\eta_0\tau}{\sqrt{2}\sigma_h}\right)+\mathrm{erf}\left(\frac{\delta}{\sqrt{2}\sigma_h}\right)\right)\end{array}\right].$$

Now we integrate over δ',

$$\Pr\left(\text{surface doesn't cross the ray } a\tau+\delta \text{ in } (0,\tau)\,|\delta\right) =$$
$$\int \Pr\left(\begin{array}{c}\text{surface doesn't cross the ray} \\ a\tau+\delta \text{ in } (0,\tau)\,|\delta,\delta'\end{array}\right) p(\delta')\,d\delta'$$
$$= \left(\int_{M_v} p(n)\,dn\right)\Pr\left(\begin{array}{c}\text{surface doesn't cross the ray} \\ a\tau+\delta \text{ in } (0,\tau)\,|\delta,\delta' \in M_v\end{array}\right)$$
$$= \left(\int_{M_v} p(n)\,dn\right)\exp\left[\kappa(\sigma,\eta_0)\left(\begin{array}{c}-\mathrm{erf}\left(\frac{\delta+\eta_0\tau}{\sqrt{2}\sigma_h}\right)+ \\ \mathrm{erf}\left(\frac{\delta}{\sqrt{2}\sigma_h}\right)\end{array}\right)\right],$$

where M_v is the set of surface normals that have a positive dot product with the viewing direction. Therefore,

$$\kappa(\sigma,\eta_0) = \left(\frac{1}{\sqrt{2\pi}}\frac{\sigma}{\eta_0}e^{-\frac{1}{2}\frac{\eta_0^2}{\sigma^2}} - \frac{1}{2}\left(1-\mathrm{erf}\left(\frac{\eta_0}{\sqrt{2\sigma^2}}\right)\right)\right).$$

References

[1] P. Beckman, "Shadowing of random rough surfaces," *IEEE Trans. Antennas Propag.*, vol. 13, p. 384, 1965.

[2] R. Brockelman and T. Hagfors, "Note on the effect of shadowing on the backscattering of waves from a random rough surfaces," *IEEE Trans. Antennas Propag.,* vol. 14, p. 621, 1966.

[3] K. J. Dana, B. van Ginneken, S. K. Nayar and J. J. Koenderink, "Reflectance and texture of real-world surfaces," *IEEE Conference on Computer Vision and Pattern Recognition (CVPR)*, pp. 151-157, 1997.

[4] K. J. Dana and S. K. Nayar, "Histogram model for 3D textures," *IEEE Conference on CVPR*, pp. 618-624, 1998.

[5] K. J. Dana, B. van Ginneken, S. K. Nayar and J. J. Koenderink, "Reflectance and texture of real-world surfaces," *ACM Transactions on Graphics*, pp. 1-34, vol. 18, no. 1, January 1999.

[6] J. S. De Bonet and P. Viola, "Texture recognition using a non-parametric multi-scale statistical model," *IEEE Conference on CVPR*, pp. 641-647, 1998.

[7] J. J. Koenderink and A. J. van Doorn, "Illuminance texture due to surface mesostructure," *J. Optical Soc. Am. A*, vol. 13 pp. 452-463, 1996.

[8] J. Krumm and S. A. Shafer, "Texture segmentation and shape in the same image," *IEEE Conference on Computer Vision*, pp. 121-127, 1995.

[9] T. Leung and J. Malik, "On perpendicular texture or: Why do we see more flowers in the distance," *IEEE Conference on CVPR*, pp. 807-814, 1997.

[10] J. Malik and R. Rosenholtz, "Computing local surface orientation and shape from texture for curved surfaces," *International Journal of Computer Vision*, vol. 23, no.2, pp.149-168, 1997.

[11] M. A. S. Patel and F. S. Cohen, "Shape from texture using Markov random field models and stereo-windows," *IEEE Conference on CVPR*, pp. 290-305, 1992.

[12] R. W. Picard, T. Kabir and F. Liu, "Real-time recognition with the entire Brodatz texture database," *IEEE Conference on CVPR*, pp. 638-639, 1993.

[13] B. Smith, "Geometrical shadowing of randomly rough surfaces," *IEEE Trans. Antennas Propag.*, p. 668, vol. 15, 1967.

[14] M. Stavridi and J. J. Koenderink, "Surface bidirectional reflection distribution function and the texture of bricks and tiles," *Applied Optics*, vol. 36, no. 16, p. 3717, 1997.

[15] P. Suen and G. Healey, "Analyzing the bidirectional texture function," *IEEE Conference on CVPR*, pp. 753-758, 1998.

[16] B. J. Super and A. C. Bovik, "Shape from texture using local spectral moments," *IEEE Transactions on Pattern Analysis and Machine Intelligence*, vol. 17, pp. 333-343, 1995.

[17] B. van Ginneken, J. J. Koenderink, and K. J. Dana, "Texture histograms as a function of irradiation and viewing direction," *IJCV-to appear 1999.*

[18] L. Wang and G. Healey, "Illumination and geometry invariant recognition of texture in color images," *IEEE Conference on CVPR*, pp. 419-424, 1996.

[19] R. Wagner, "Shadowing of randomly rough surfaces," *Journal of the Acoustical Society of America*, p. 138, vol. 41, 1967.

[20] P. Welton, K. Hawker, and H. Frey, "Experimental shadowing measurements on randomly rough surfaces," *Journal of the Acoustical Society of America*, vol. 54, no. 2, p. 446, 1973.